ON PID CONTROL FOR NONLINEAR ACTIVE VEHICLE SUSPENSION SYSTEMS

O.A. Dahunsi *, J.O. Pedro † and M.M. Ali ‡

Study Group participants

A.O. Adewumi, M.A. Arasomwan, L.O. Joel, I.C. Obagbuma and M.O. Olusanya

Abstract

In spite of the superior performance of active vehicle suspension system (AVSS), its implementation on a large commercial scale is delayed because of challenges related to controller design and hardware. Other controllers employed present implementation problems because of computational challenges. PID feedback control loops with a cascade of two other PID sub-loops for force control and spool valve displacement control. The additional PID controllers (in the inner loops) did not only help in stabilizing the actuator dynamics, but they also increased the chances of better AVSS performance by the addition of extra tuning variables. The control voltage, spool-valve displacement and suspension travel signals were within their allowable limits. However, the maximum allowable actuator force value was marginally exceeded at the peak of the first hump. Initial steady state levels were restored $0.5s$ after each disturbance.

*School of Mechanical, Industrial and Aeronautical Engineering, University of the Witwatersrand, Johannesburg, South Africa. *email: Olurotimi.Dahunsi@students.wits.ac.za*

†School of Mechanical, Industrial and Aeronautical Engineering, University of the Witwatersrand, Johannesburg, South Africa. *email: Jimoh.Pedro@wits.ac.za*

‡School of Computational and Applied Mathematics, Faculty of Science and Transnet Centre of System Engineering (TCSE), Faculty of Engineering and Built Environment, University of the Witwatersrand, Johannesburg, South Africa. *email: Montaz.Ali@wits.ac.za*

1 Introduction

There is a growing demand for more comfortable ride in vehicles without sacrificing improved performance. The quality of a vehicle's suspension influences its driving safety, ride comfort, vehicle handling and road holding capacity [1, 2, 3, 4]. Rapid advances in the field of electronics, instrumentation and control have facilitated the implementation of active vehicle suspension systems in commercial, luxury, military and construction vehicles today [5, 6]. The biggest advantage that active suspension has over other suspension types is its ability to provide better compromise between the conflicting design parameters of a vehicle suspension system [3, 4, 7, 8].

Controller design works for AVSS are well documented. Methods employed already cut across the entire spectrum of control techniques. It includes optimal control methods that are relatively well developed, robust and their stability is readily established and nonlinear and intelligent control methods [9, 10].

The objective of most linear optimal control methods employed in AVSS is to obtain optimal feedback gains needed to minimise the chosen performance objectives. There are several multiobjective combinations of various optimal control methods that have been proposed with improved performance results and robustness. Moreover, the multiobjective control problem yields a non-convex optimisation problem that is difficult to solve. Similarly, the fixed optimal gains cannot be adjusted in the face of varying operating conditions like changing road disturbance inputs [11, 12].

Feedback linearization, backstepping and sliding mode controls are the popular nonlinear control schemes that have been employed in AVSS design. Their control performances were good in the face of the inherent nonlinear characteristic of AVSS, coupled with challenges related to its parametric uncertainties. They however suffer setback at the point of implementation because of degradation of system performance due to chattering. While several innovations have been employed to handle this challenge, the processes brings in complications in the course of controller design [1, 13].

PID control remains the most employed industrial controller because of its simple structure and relative ease of tuning either intuitively or by available tuning methods [14, 15, 16, 17]. Although controllers sacrifice this simplicity and computational ease for better performance, the prospect of better or similar level of performance exist for PID when combined with other controllers or tuned using computational intelligence techniques. These combinations can also improve its robustness to parameter variation and better tuning of the high loop gains [16,

18, 19, 20]. Finally, PID is more effective at adjusting system parameters like overshoot, rise and settling time [18, 21].

Even although electrohydraulic actuators remain the most viable source of actuator force for AVSS applications because of advantages like lower cost, high power-to-weight ratio, fast response, high stiffness and good load bearing capability, the dynamics due to its highly coupled interaction with the suspension is highly nonlinear. Many of the documented works neglected actuator dynamics for this reason [22, 19, 23, 24]. Some documented works have shown that introduction of a sub-loop for the feedback control of the command force contributes immensely to the stability and tracking in the presence of deterministic road disturbances [22, 21, 24].

In this work, PID feedback control loops are employed for disturbance rejection (originating from the uneven road terrain), actuator force control and actuator spool-valve position control. The effectiveness of the electrohydraulic actuator depends on accurate positioning of its spool valve. In the past, spool valve displacement has been ignored because of instrumentation and cost challenges. Servo-valve assemblies with mounted miniaturised or embedded Linear Variable Differential Transformer (LVDT) are now available [25, 26, 27].

The rest of the paper is structured as follows. The second section presents a brief description of the physical, mathematical and road disturbance input models. The third section highlights the system specifications and evaluation criteria, while the fourth section presents the controller design. The fifth section presents the discussion of results and is followed by the concluding remarks in the last section.

2 System modelling

2.1 Description of physical model

Figure 1 presents the generic active vehicle suspension system (AVSS) feedback control loop. The system consists of a controller issuing the command input to the actuator to generate a manipulating signal.

AVSS responds dynamically to road disturbance inputs by inducing relative motion between the body and the wheel through the force generated by the servo-hydraulic actuator. Obtaining the appropriate control voltage for the actuator includes an optimal trade-off between the design objectives in the presence of road disturbance inputs. The success of this process yields a suspension system

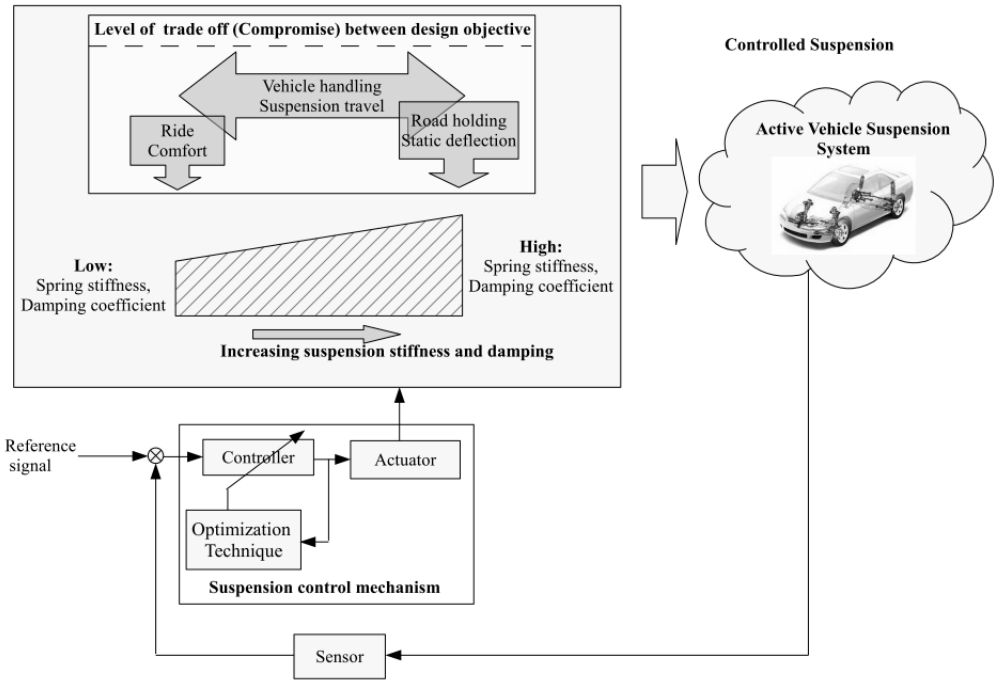

Figure 1: AVSS feedback control loop

that is adaptive to the road disturbance and other operating conditions.

The physical system used for this investigation is a 2DOF, quarter-car independent suspension model shown in Figure 2. This model readily captures the body heave and wheel hop vibration mode. The sprung mass (chassis) is represented by m_s, unsprung mass (wheel) by m_u, k_s and k_t are the suspension and wheel stiffnesses respectively, b_s is the damping coefficient of the suspension system, F is the actuator force, x_1 and x_2 are the vertical displacements of the chassis and wheel respectively, while w is the road disturbance input.

2.2 Mathematical model

The controlled variable is represented by the suspension travel $(x_1 - x_2)$, $\ddot{x}_1$ is the heave acceleration which signifies the ride comfort and $(x_2 - w)$ represents the wheel deflection which characterizes road holding quality.

Application of Newton's law to the quarter-car model shown in Fig. 2 yields

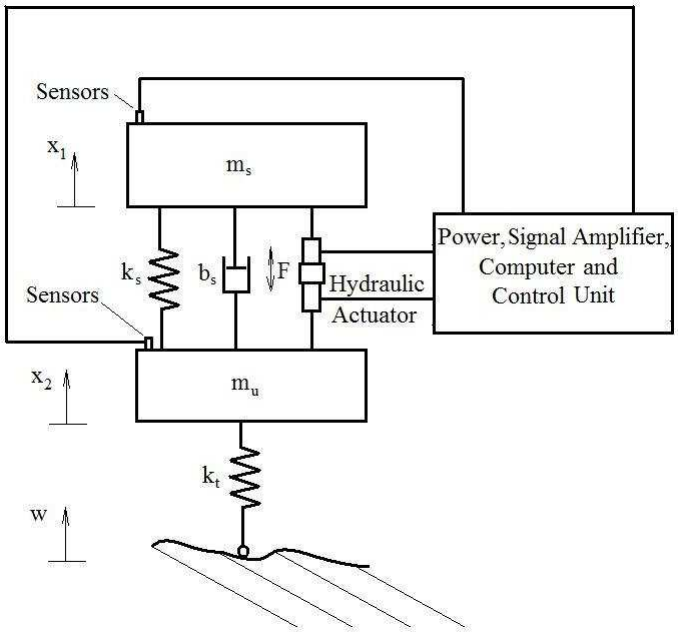

Figure 2: Quarter-car model

the following nonlinear governing equations [20, 28]:

$$\dot{x}_1 = x_3 \ , \tag{2.1}$$

$$\dot{x}_2 = x_4 \ , \tag{2.2}$$

$$\begin{aligned} m_s\dot{x}_3 = {} & k_s^l(x_2 - x_1) + k_s^{nl}(x_2 - x_1)^3 \\ & + b_s^l(x_4 - x_3) - b_s^{sym}|x_4 - x_3| \\ & + b_s^{nl}\sqrt{|x_4 - x_3|}sgn(x_4 - x_3) - Ax_5 \ , \end{aligned} \tag{2.3}$$

$$\begin{aligned} m_u\dot{x}_4 = {} & -k_s^l(x_2 - x_1) - k_s^{nl}(x_2 - x_1)^3 \\ & - b_s^l(x_4 - x_3) + b_s^{sym}|x_4 - x_3| \\ & - b_s^{nl}\sqrt{|x_4 - x_3|}sgn(x_4 - x_3) \\ & - k_t(x_2 - w) + Ax_5 \ , \end{aligned} \tag{2.4}$$

$$\dot{x}_5 = \gamma\Phi x_6 - \beta x_5 - \alpha A(x_3 - x_4) \ , \tag{2.5}$$

$$\dot{x}_6 = \frac{1}{\tau}(-x_6 + u) \ , \tag{2.6}$$

where

$$\alpha = \frac{4\beta_e}{V_t}\ , \qquad \beta = \alpha C_{tp}\ , \qquad \gamma = C_d S\sqrt{\frac{1}{\rho}}\ , \qquad \Phi = \phi_1 \times \phi_2\ ,$$
$$\phi_1 = sgn[P_s - sgn(x_6)x_5]\ , t \qquad \phi_2 = \sqrt{|P_s - sgn(x_6)x_5|}\ ,$$

Figure 3 represents the hydraulic actuator mounted between the sprung and the unsprung masses. The hydraulic fluid flow rates Q_u and Q_l into the upper and lower chambers of the cylinder determine the actuator force generated.

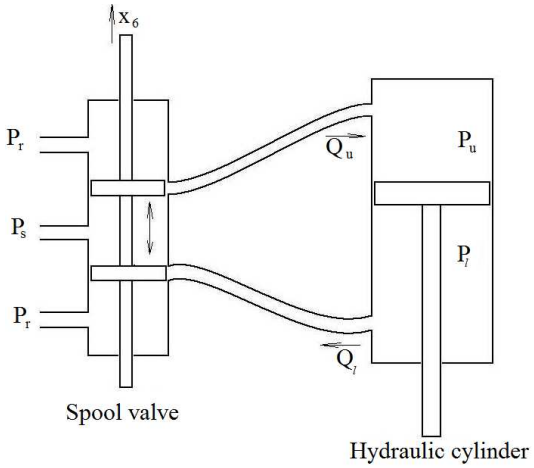

Figure 3: Schematic of the Double Acting Hydraulic Strut

The electro-hydraulic system is modelled as a first order dynamic system with a time constant τ. Supply voltage of range $\pm 10 volts$ is supplied to the servo-valves as control input to limit the suspension travel to $\pm 10 cm$ [29].

The area of the piston is A, x_3 and x_4 are the vertical velocities of the sprung and unsprung masses respectively, x_5 is the pressure drop across the piston, x_6 is the servo-valve displacement, P_s is the supply pressure into the hydraulic cylinder, P_r is the return pressure from the hydraulic cylinder, P_u and P_l are the oil pressure in the upper and lower portion of the cylinder, V_t is the total actuator volume, β_e is the effective bulk modulus of the system, Φ is the hydraulic load flow, C_{tp} is the total leakage coefficient of the piston, C_d is the discharge coefficient, S is the spool-valve area gradient and ρ is the hydraulic fluid density.

The suspension spring and damping forces have linear and nonlinear components. The spring constant k_s^l and damping coefficient b_s^l affect the spring force

and damping force in a linear manner. The parameter b_s^{sym} contributes an asymmetric characteristics to the overall behaviour of the damper. The parameters k_s^{nl} and b_s^{nl} are responsible for the nonlinear components of the spring and damper forces respectively.

2.3 Road disturbance input models

The performance of the suspension system is evaluated at the vehicle travelling speed of $40km/h$ in the presence of a road disturbance input with sinusoidal profile, wavelength of $5m$ and amplitude of $11cm$. The profile of the hump is modelled by Equation 2.7.

$$w(t) = \begin{cases} \frac{a_1}{2}(1 - cos\frac{2\pi Vt}{\lambda}) , & 1 \leq t \leq 1.25 , \\ \frac{a_2}{2}(1 - cos\frac{2\pi Vt}{\lambda}) , & 3 \leq t \leq 3.25 , \\ 0 , & \text{otherwise,} \end{cases} \tag{2.7}$$

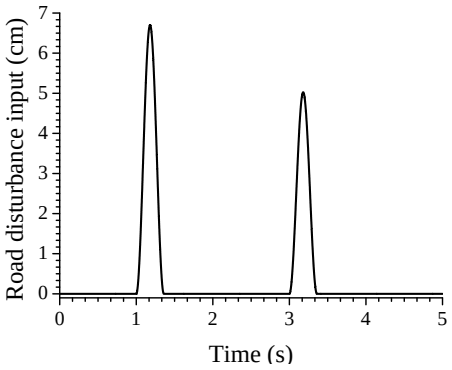

Figure 4: Road disturbance input profile - deterministic

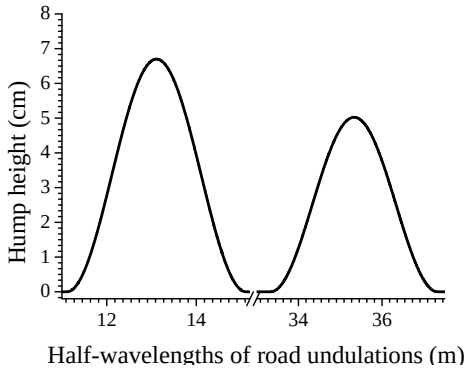

Figure 5: Lateral view of road disturbance input profile - deterministic

where a is the bump height, V is the vehicle's velocity in a straight line and λ is the half wavelength of the sinusoidal road undulation. The values for the system parameters are provided in Table 1.

Table 1: Parameters of the Quarter - Car Model [28, 25]

Parameters	Value	Parameters	Value
Sprung mass, m_s	290kg	Suspension stiffness (linear), k_s^l	$2.35 * 10^4 N/m$
Unsprung mass, m_u	40kg		
Tyre stiffness,k_t	$1.9 \times 10^5 N/m$	Suspension stiffness (nonlinear), k_s^{nl}	$2.35 * 10^6 N/m$
Bump height, a	$0.11m$		
Piston area, A	$3.35 \times 10^{-4} m^2$	Suspension damping (linear), b_s^l	$700 Ns/m$
Actuator time constant, τ	$3.33 \times 10^{-2} sec$	Suspension damping (nonlinear), b_s^{nl}	$400 Ns/m$
Supply pressure (P_s)	$10,342,500 Pa$	Suspension damping (asymmetrical), b_s^{sym}	$400 Ns/m$
Vehicle speed (V)	$30 ms^{-1}$		
Disturbance half wavelength (λ)	$5m$	Actuator parameter (α)	4.515×10^{13}
		Actuator parameter (β)	1
		Actuator parameter (γ)	1.545×10^9

3 System performance specification and evaluation

3.1 Performance specifications

The following characteristics are required of the AVSS controller in a bid to meet the set performance objectives:

1. **Nominal stability**: The closed-loops should be nominally stable. Stability in the inner loop is enhanced through a force feedback loop. The enhanced stability of the actuator dynamics should improve the overall system stability.

2. **Disturbance rejection**: The controller should demonstrate good low frequency disturbance attenuation.

3. **Good command following**: The suspension travel response of the AVSS is examined in the presence of the deterministic road inputs shown in Figures 4 and 5. The controller should be able to keep the steady-state error as close to zero as possible.

4. **Suspension travel**: It is constrained to physical limits to avoid damage due to topping and bottoming. Thus it is not to exceed $\pm 0.1m$ [25].

5. The **control voltage** is also limited to $\pm 10volts$.

6. The maximum **actuator force** must be less than the static weight of the vehicle, that is $F_{hyd} < m_s g$.

7. For good **road holding** the dynamic load that is transmitted through the road should not be larger than the static weight of the vehicle. The dynamic load is normalized with the static weight of the vehicle.

8. **Ride comfort**: This is quantified using the vehicle body acceleration in the vertical direction. The vertical acceleration of the vehicle body needs to be minimal for good ride comfort, especially within the low frequency band of 0.1 to $10Hz$. The peak sprung mass acceleration: $\ddot{x}_1 < 4.5m/s^2$ [30, 31, 32].

3.2 Optimal trade-off among performance criteria

The objective function employed in the tuning of the controller gains is presented in Equation 3.1. It is designed to minimise the suspension travel, y, actuator force, F, sprung mass acceleration, $\ddot{x}_1$, actuator spool-valve displacement, x_6, control voltage, u, and wheel deflection, $(x_2 - w)$. In this way, ride comfort and road holding are improved while control voltage and actuator force are kept as small as possible. The objective function is

$$J = \frac{1}{T}\int_0^T \left[\left(\frac{y}{y_{max}}\right)^2 + \left(\frac{F}{F_{max}}\right)^2 + \left(\frac{\ddot{x}_1}{\ddot{x}_{1\,max}}\right)^2 + \left(\frac{\dot{x}_6}{\dot{x}_{6\,max}}\right)^2 + \left(\frac{u}{u_{max}}\right)^2 + \left(\frac{(x_2 - w)}{(x_2 - w)_{max}}\right)^2\right] dt\,. \tag{3.1}$$

4 Controller design

Implementation of the PID controlled arrangement was carried out in the $MATLAB^{®}$ $/SIMULINK^{®}$ environment. The desired controlled output, y, is the suspension travel. The control arrangement for AVSS is shown in Figure 6. Although

each controller must be tuned independently, changes in any of the controller gains affect the overall performance of the system, thereby making it necessary to re-tune the other controllers.

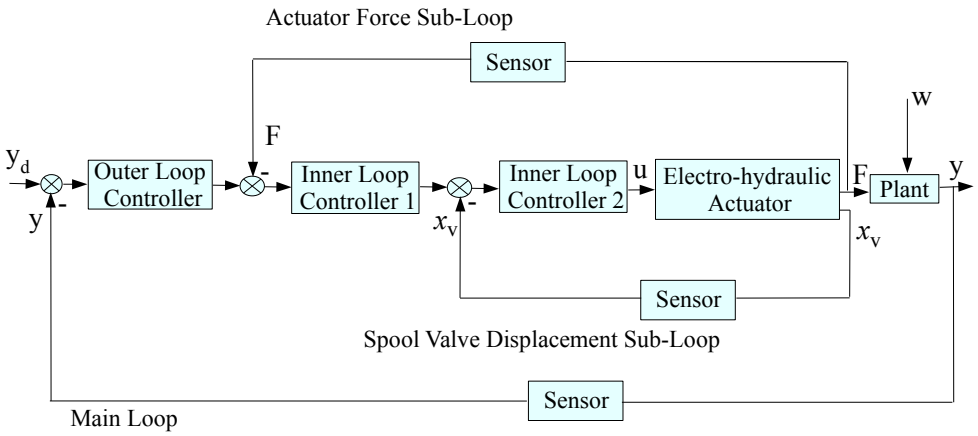

Figure 6: AVSS multi-loop PID control configuration

The PID-controlled signal consist of the K_P term which is proportional to the error signal e, K_I which is proportional to the integral of the error signal and K_D which is proportional to the derivative of the error signal. Therefore, the PID control law is given by:

$$u(t) = K_P e(t) + K_I \int e(t)dt + K_D \frac{d}{dt} e(t) \ , \tag{4.1}$$

where $e(t) = y_d(t) - y(t)$. The reference signal $y_d(t)$ is set to zero. Therefore the objective is to design a control law for $u(t)$ such that $e(t) \to 0$ as $t \to \infty$.

The controllers were tuned using the Ziegler-Nichols tuning criterion on the basis of 0.25 decay ratio and understanding of the system characteristics. Further fine tuning required was done manually since PID controllers tend to generate too high control inputs leading to saturation [33]. Table 2 presents the selected gains for the three controllers. The three controllers required the same gain value for their integral component. The values for the integral and derivative components of the controllers were also marginal when compared to those of the proportional gains.

Table 2: PID tuning parameters

	PID Gains		
	K_P	K_I	K_D
Main loop	100	1×10^{-6}	1×10^{-6}
Spool valve displacement sub-loop	7×10^{-3}	1×10^{-6}	1×10^{-6}
Actuator force sub-loop	3.87×10^{-4}	1×10^{-6}	1×10^{-8}

5 Simulation results and discussion

The control problem being solved was set up as a disturbance rejection problem. The disturbance input consisted of the twin humps shown in Figures 4 and 5. The control objective was to minimise or eliminate deviation from the pre-set suspension travel value in spite of the disturbance input. The vehicle velocity was $40km/h$.

A multi-loop PID control scheme was set-up as shown in Figure 6 and numeric simulation was executed in the $MATLAB^{®}$ environment. The actuator force generated was as a variable but preset control input of $\pm 10\, volts$: It was supplied to the solenoid valve of the electrohydraulic actuator in response to the disturbance input.

Time histories of the AVSS's response are combined into Figure 7 where SVD stands for the spool-valve displacement, AF represents the actuator force, RDI represents the road disturbance input, CV represents the control voltage, NWDL represents the normalized wheel dynamic load, ST represents the suspension travel and BA represents the vehicle body acceleration. The range of values for the spool-valve displacement, control voltage and the suspension travel are well below the maximum allowable limits of $\pm 1cm$, $\pm 10\, volts$ and $\pm 10cm$ respectively. The effects of the road disturbance input are clearly evident in Figure 7. The controllers were able to return the responses back to the initial steady-state values within $0.5sec$ of the occurrence of the disturbance inputs.

The peak vehicle body acceleration values ranged between $1.41ms^2$ and $1.11ms^2$, the normalized wheel dynamic load ranged between 1.16 and 1.45, and the actuator force ranged between $3.34kN$ (which is marginally above the maximum allowable value) and $3.23kN$ (which is marginally below the maximum allowable value).

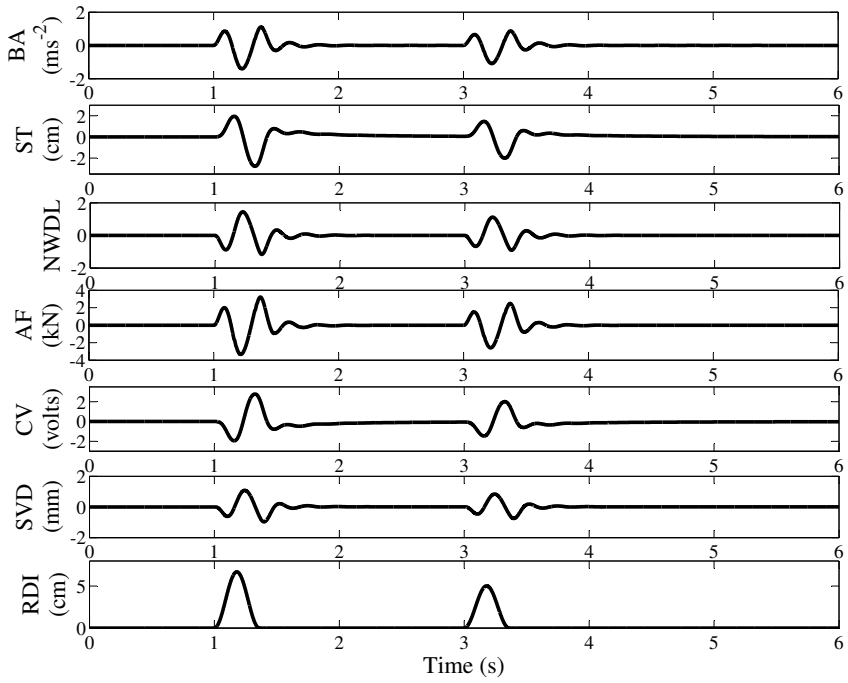

Figure 7: Time history of the AVSS responses to deterministic road excitations

6 Conclusions

The PID controller has been designed for a nonlinear AVSS application. Two inner PID control loops have been employed to stabilize the actuator dynamics and enhance the main regulatory control of the outer loop. All the responses were within the stipulated ranges except for the actuator force which exceeded the range marginally.

The popularity of PID control in terms of industrial applications cannot be ignore. Its structure and tuning are relatively simple thus making it more readily applicable in cases where multiple or cascaded feedback control loops are required. We have demonstrated that introducing an additional PID control loop increases the tuning options in addition to further stabilising the actuator dynamics. As a consequence, the number of elements to be tuned is increased and this may be cumbersome unless some autotuning method is adopted.

References

[1] Kaddissi, C., Saad, M. and Kenne, J.P. Interlaced back stepping and integrator forwarding for nonlinear control of an electro-hydraulic active suspension. *Journal of Vibration and Control*, **15** (2009), 101–131.

[2] Fischer, D. and Isermann, R. Mechatronic semi-active and active vehicle suspensions. *Control Engineering Practice*, **12** (2004), 1353–1367.

[3] Hrovat, D. Survey of advanced suspension developments and related optimal control applications. *Automatica*, **33** (1997), 1781–1817.

[4] ElMadany, M.M. and Qarmoush, A.O. Dynamic analysis of a slow-active suspension system based on a full-car model. *Journal of Vibration and Control*, **17** (2011), 39–53.

[5] Gysen, B.L.J., Paulides, J.J.H., Janssen, J.L.G. and Lomonova, E.A. Active electromagnetic suspension system for improved vehicle dynamics. *IEEE Transactions on Vehicular Technology*, **59** (2010), 1156–1163.

[6] Koch, G., Fritsch, O. and Lohmann, B. Potential of low bandwidth active suspension control with continuously variable damper. *Proceedings of the 17th World Congress, The International Federation of Automatic Control (IFAC)*, Seoul, South Korea, July 2008, pp 3392–3397.

[7] Pedro, J.O. H_2- *LQG/LTR* controller design for active suspension systems. *R and D Journal of the South African Institution of Mechanical Engineering*,**23** (2007), 32–41.

[8] Xue, X.D., Cheng. K.W.E.., Zhang, Z., Lin, J.K., Wang, D.H., Bao, Y.J., Wong, M.K. and Cheung, N. Study of art of automotive active suspensions. In *Proceedings of the 4th International Conference on Power Electronics Systems and Applications (PESA)*, Hong Kong, China, June 2008, pp 1–6.

[9] Cao. J., Liu, H., Li, P. and Brown, D. State of the art in wheel active suspension adaptive control systems based on intelligent methodologies. *IEEE transactions of Intelligent Transportation Systems*, **9** (2008), 392–405.

[10] Cao, D., Song, X. and Ahmadian, M. Editor's perspectives: Road vehicle suspension design, dynamics and control. *Vehicle System Dynamics*, **49** (2011), 3–28.

[11] Du, H. and Zhang, N. Multi-objective static output feedback control design for vehicle suspensions. *Journal of System Design and Dynamics*, **2** (2008), 228–239.

[12] Lu, J. and DePoyster, M. Multi-objective optimal suspension control to achieve integrated ride and handling performance. *IEEE Transactions on Control Systems Technology*, **10** (2002), 807–827.

[13] Li, T.H.S., Huang, C.J. and Chen, C.C. Almost disturbance decoupling and tracking control of MIMO nonlinear system subject to feedback linearization and a feed-forward neural network: Application to half-car active suspension system. *International Journal of Automotive Technology*, **11** (2010), 581–592.

[14] Giovanni, L. Predictive feedback control: An alternative to proportional-integral-derivative control. *Proceedings of the Institute of Mechanical Engineers, Part I: Journal of Systems and Control Engineering*, **223** (2009), 901–917.

[15] Ang, K.H. and Li, Y. PID control system analysis , design and technology. *IEEE Transactions on Control Systems Technology*, **13** (2005), 558–576.

[16] Goncalves, E.N., Palhares, R.M. and Takahashi, R.H.C. A novel approach for H_2/H_∞ robust PID synthesis for uncertain systems. *Journal of Process Control*, **18** (2008), 19–26.

[17] Gao, Z. From linear to nonlinear control means: A practical progression. *ISA Transactions*, **41** (2002), 177–189.

[18] Cetin, S. and Akkaya, A.V. Simulation and hybrid fuzzy-PID control for positioning of a hydraulic system. *Nonlinear Dynamics*, **65** (2010), 465–476.

[19] Dahunsi, O.A., Pedro, J.O. and Nyandoro, O.T. System identification and neural network based PID control of servo-hydraulic vehicle suspension systems. *Transactions of the South African Institute of Electrical Engineersion (SAIEE), Africa Research Journal (ARJ)*, **101** (2010), 93–105.

[20] Pedro, J.O., Dangor, M., Dahunsi, O.A. and Ali, M.M. CRS and PS - optimised PID controller for nonlinear, electro-hydraulic suspension. In *Proceedings of the 9th Asian Control Conference, Istanbul, Turkey, June* 2013, pp 1251–1257.

[21] Ekoru, J.E.D. and Pedro, J.O. Proportional-integral-derivative control of nonlinear half-car electro-hydraulic suspension systems. *Journal of Zhejiang University - Science A (Applied Physics & Engineering)*, **14** (2013), 401–416.

[22] Chantranuwathana, S. and Peng, H. Adaptive robust force control for vehicle active suspensions. *International Journal of Adaptive Control and Signal Processing*, **18** (2004), 83–102.

[23] Ekrou, J.E.D., Dahunsi, O.A. and Pedro, J.O. PID control of a nonlinear half-car active suspension via force feedback. In *Proceedings of the 2011 IEEE AFRICON*, Livingstone, Zambia, 2011, .

[24] Fateh, M.M. and Alawi, S.S. Impedance control of an active suspension system. *Mechatronics*, **19** (2005), 134–140.

[25] Fialho, I. and Balas, G.J. Road adaptive active suspension using linear parameter-varying gain-scheduling. *IEEE Transactions on Control Systems Technology*, **10** (2002), 43–54.

[26] Ayalew, B and Kulakowski, B.T. Modeling supply and return line dynamics for an electro-hydraulic actuation system. *ISA Transactions*, **44** (2005), 329–343.

[27] Li, P.Y. and Yuan, Q. Flux observer for spool displacement sensing in self-sensing push-pull solenoids. In *Proceedings of the 6th International Conference on Fluid Power Transmission and Control (ICFP)* 2005, Hanzhou, China, pp 1–5.

[28] Gasper, P., Szaszi, I. and Bokor, J. Active suspension design using linear parameter varying control. *International Journal of Autonomous Systems (IJVAS)*, **1** (2003), 206–221.

[29] Du, H. and Zhang, N. Static output feedback control for electro-hydraulic active suspensions via T-S fuzzy model approach. *Journal of Dynamic Systems, Measurement and Control: Transactions of ASME*, **131** (2009), pp 051004–1–051004–11.

[30] Griffin, M.J. Discomfort from feeling vehicle vibration. *Vehicle Systems Dynamics*, **45** (2007), 679–698.

[31] European Commission. Directive 2002/44/EC of the European Parliament and the Council of 25 June 2002 on the minimum health and safety requirements regarding the exposure of workers to the risk arising from physical agents *(vibration)*. Official *Journal of the European Communities, Luxembourg*, 2002.

[32] ISO 2631. Mechanical Vibration and Shock - Evaluation of Human Exposure to Whole-Body Vibration - Part 1 : General Requirements. *International Organization for Standardization*, Geneva, Switzerland, 2003.

[33] Astrom, K.J. and Hagglund, T. The future of PID control. *Control Engineering Practice*, **9** (2001), 1163–1175.